

## Investigation on the capacity of deep learning to handle uncertainties in remaining useful life prediction

Khanh T. P. Nguyen<sup>1</sup>, Zeina Al Masry<sup>2</sup>, Kamal Medjaher<sup>1</sup>, and Noureddine Zerhouni<sup>2</sup>

<sup>1</sup>Laboratoire Génie de Production, INP-ENIT, Université de Toulouse, France.

E-mail: thi-phuong-khanh.nguyen, kamal.medjaher@enit.fr

<sup>2</sup>SUPMICROTECH, CNRS, institut FEMTO-ST, 24 rue Alain Savary, Besançon, F-25000, France.

E-mail: zeina.almasry@femto-st.fr, noureddine.zerhouni@femto-st.fr

Remaining useful life (RUL) prediction is subjected to multiple uncertainty sources, such as measurement errors, operating conditions, and model representation capability. The quantification of the prediction uncertainty is important for assisting decision-making. In literature, stochastic processes have proven their efficiency in handling uncertainties in prognostics by providing RUL distribution. However, they have limitations in their adaptability to capture the dynamic behaviors of complex systems. To address this issue, it is recommended to employ deep learning (DL) methods that usually generate point-wise RUL predictions instead of RUL distribution. Therefore, the objective of this work is to investigate the capacity of DL methods to manipulate uncertainty in RUL predictions. Particularly, the probabilistic deep learning (PDL) framework is used to predict the RUL distribution instead of a point-wise RUL value. The obtained results by PDL are compared with the analytic solutions of the stochastic processes to highlight the uncertainty management capacity of PDL.

*Keywords:* Stochastic processes, Prognostics and Health Management, Deep Learning, RUL prediction, Uncertainty management.

### 1. Introduction

Nowadays, the rapid growth of modern technologies in Internet of Things (IoT) and sensing platforms is enabling a wide range and a high quantity of condition monitoring data. This has opened up many development prospects for Prognostics and Health Management (PHM) both in the research community and within industry. One of PHM's main tasks is prognostics, i.e. Remaining Useful Life (RUL) predictions to prevent unexpected system downtime. In literature, model-based prognostic approaches use explicit mathematical models or stochastic processes to model degradation evolution over time and predict the RUL distribution Kahle et al. (2016); Nguyen et al. (2018); Zhang et al. (2021). However, with the increasing complexity of modern industrial systems, it is challenging to obtain models of their degradation. Alternatively, data-driven methods provide an alternative to model-based approaches by using monitoring data to learn system behavior and degradation trends. With the increasing availability of large amounts of data

in industry, data-driven approaches are promising for developing accurate prognostic models, even for complex systems. The performance of traditional methods, e.g. support vector machine, and logistic regression, strictly depends on hand-crafted features Nguyen et al. (2022). Alternatively, deep learning (DL) methods, which allow automatic extracting and creating useful features by themselves without expert knowledge, become one of the most popular trends in recent studies Nguyen and Medjaher (2019). However, they generally provide a precise value without a quantification of the output uncertainty and require a large set of observations to train the model.

In practice, as prognostics deals with prediction of future system behavior, numerous sources of uncertainties exist in RUL predictions Liu et al. (2019). Therefore, managing uncertainty is crucial for effective prognostics. Recent studies have explored probabilistic deep learning (PDL) to quantify prognostic uncertainties Nguyen et al. (2022); Dhada et al. (2023). However, to our

knowledge, no previous studies have compared the capacity of PDL to handle prognostic uncertainties against stochastic processes. This study aims to address this gap. To do that, we generate degradation data using multiple stochastic processes, such as Wiener and Gamma processes with varying levels of variation. PDLs are trained on this data to predict RUL, and the results are compared with analytic solutions from the stochastic process to assess the advantages and disadvantages of each technique.

The remainder of the paper is as follows. Section 2 presents the theoretical background of the used techniques. In Section 3, we provide the description of the used methodology to investigate the capacity of PDLs to handle uncertainty. Section 4 shows the numerical results. Finally, a conclusion and a comparative table are presented in Section 5.

## 2. Theoretical backgrounds

### 2.1. Uncertainty management by Gamma processes

Gamma process is one of the most popular stochastic process that has been used to model stochastic deterioration (see van Noortwijk (2009)). It is a continuous-time process and it is well adapted for modeling accumulative (non-decreasing) deterioration such as corrosion, erosion, and crack growth.

**Definiiton of gamma process.** Let  $A : \mathbb{R}_+ \rightarrow \mathbb{R}_+$  be a measurable, increasing and right-continuous function with  $A(0) = 0$  and  $b > 0$ . A stochastic process  $X$  is said to be gamma process  $Y = (Y_t)_{t \geq 0} \sim \Gamma(A(\cdot), b)$ , with  $A(\cdot)$  as shape function and  $b$  as scale parameter, if (1)  $X_0 = 0$  almost surely, (2) the increments are independent and non-negative, and (3) the increments are gamma distributed.

The probability density function of an increment  $X_t - X_s$  (with  $0 < s < t$ ) is given by

$$f(x) = \frac{b^{A(t)-A(s)}}{\Gamma(A(t) - A(s))} x^{A(t)-A(s)-1} \exp(-bx),$$

$$\forall x \geq 0 \text{ and where } \Gamma(A(t) - A(s)) = \int_0^\infty y^{A(t)-A(s)-1} \exp(-y) dy.$$

The mean and variance of  $Y_t$  are given by:  $\mathbb{E}[X_t] = \frac{A(t)}{b}$ ,  $\mathbb{V}[X_t] = \frac{A(t)}{b^2}$  for all  $t \geq 0$ .

Note that, based on the form of the shape function, the gamma process is said to be:

- Homogeneous if  $A(t)$  is a linear function in  $t$ :  $A(t) = at$ ,  $a > 0$ .
- Non-homogeneous if  $A(t)$  is a non-linear function:  $A(t) = at^c$ ,  $a > 0$ ,  $c > 0$ .

**Remaining useful life prediction.** Let  $L > 0$  denote a failure threshold. Given a degradation level  $X_t = x$  at time  $t$ , the cumulative distribution of the remaining useful life (RUL) of a gamma process is given by Paroissin and Salami (2014):

$$F_{RUL(x,t)}(u) = \frac{\Gamma(A(u+t) - A(t), (L - x_t)b)}{\Gamma(A(u+t) - A(t))}, \tag{1}$$

where  $\Gamma(\cdot, \cdot)$  is the upper incomplete Gamma function.

**Parameter estimation.** Based on the collected sample data (degradation records at observation times), the parameters of gamma process are estimated using the Maximum Likelihood Estimation (MLE). The estimates are obtained by maximizing the following log-likelihood function:

$$l = \ln \left( \prod_{i=1}^n \frac{b^{(A(t_i) - A(t_{i-1}))}}{\Gamma(A(t_i) - A(t_{i-1}))} \times \Delta X_i^{A(t_i) - A(t_{i-1}) - 1} \exp(-b \Delta X_i) \right), \tag{2}$$

where  $\Delta X_i = X_{t_i} - X_{t_{i-1}}$  for  $i = 1, \dots, n$ .

### 2.2. Deep learning for uncertainty handling

In this subsection, we introduce PDL framework to predict the parameters that characterize the RUL distribution at time  $t$  of component  $i$ . Figure 1 presents an overview of the proposed framework. It consists of the following layers:

- (1) *Input layer:* The prototype brings formalized data, represented as a 3D tensor with shape  $(n_s, n_t, m)$ , into the network for processing.

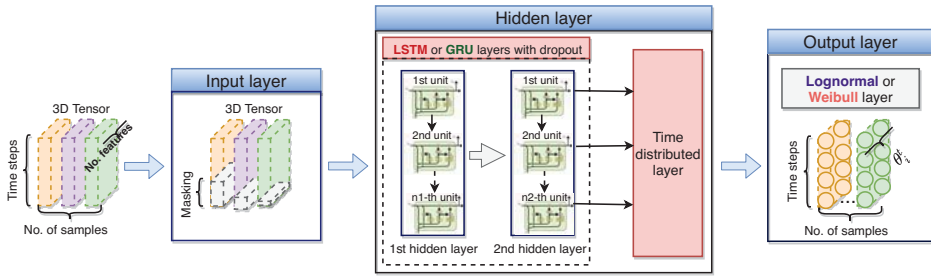


Fig. 1.: Architecture of probabilistic deep learning framework for RUL prediction.

Recall that  $\theta_i^t$  is the output vector characterizing RUL distribution of trajectory  $i$  at time  $t$ , including 2 parameter values of Lognormal ( $\mu_i^t$  and  $\sigma_i^t$ ) or Weibull distribution ( $\alpha_i^t$  and  $\beta_i^t$ ).

A **masking layer** is used during training to skip the right padding and avoid bias errors.

- (2) *Hidden layer:* It is the principal part of the network, including two DL layers and one time-distributed layer.

**For DL part,** we specifically investigate in this paper, the effectiveness of Long short-term memory (LSTM) and Gated Recurrent Unit (GRU) architectures for processing time-series data. However, it is important to note that other deep learning architectures, such as convolutional neural networks (CNNs) or Transformers, may also be used for this framework depending on the characteristics of the input data. The details of LSTM and GRU models can be consulted in the paper Hochreiter and Schmidhuber (1997) and Cho et al. (2014) respectively. These two models are widely used in prognostics due to their ability to capture long-term dependencies and handle vanishing gradient problems. They achieve this by using gates that allow the model to selectively forget or remember information over time.

To avoid the overfitting issue, the ‘‘Dropout’’ regularization technique is added to every LSTM (or GRU) layer Hinton et al. (2012). It involves randomly removing some hidden units in a neural network during training by a defined probability.

**Time distributed layer** applies the same fully-connected operation to every time step of the DL layer outputs, producing an output

vector per time step with dimensions based on the number of RUL distribution parameters in the output layer. For example, if the RUL follows a Lognormal distribution, the time-distributed layer will have 2 units representing  $\mu$  and  $\sigma$ .

- (3) *Output layer:* It is defined to take into account particular characteristics of RUL distribution parameters when training the model. It provides the proper parameters representing the RUL distribution instead of a point-wise RUL prediction. In this paper, the Weibull (WB) distribution and Lognormal (LN) distribution are chosen to manage the uncertainty in RUL prediction because they are commonly used to model unit lifetimes, can only take positive values, and are based on a multiplicative growth model suitable for diverse components. While we focus on these two specific distributions in this study, it is important to note that other probability distributions could also be integrated into the proposed framework by defining the output layer with the appropriate activation function and the appropriate loss function. This allows for a flexible and adaptable approach to modeling RUL distribution based on the specific needs and characteristics of different machinery and equipment. Particularly, instead of predicting a target RUL value,  $y^*$ , the proposed PDL framework will provide a couple of parameters characterizing RUL distribution to maximize the probability when

$RUL_i^t = y^*$ . For instance, if RUL follows the Lognormal distribution, the PDL framework provides two parameters  $(\mu_i^t, \sigma_i^t)$ , while it gives two parameters  $(\alpha_i^t, \beta_i^t)$  for the Weibull distribution. To do this, it is essential to define activation functions tailored to the characteristics of these parameters and a loss function designed to maximize the probability of RUL values for a given component  $i$  from its initial observation time up until the time at which its observations were recorded. The methodology for defining such activation and loss functions for Lognormal and Weibull distributions is explicated in Nguyen et al. (2022) and Dhada et al. (2023). During the training process, the PDL model's weights and biases will be iteratively adjusted to minimize the negative logarithm likelihood (NLL) function, which is expressed by the following equation, thereby obtaining optimal sets of RUL distribution parameters  $(\theta_i^t)$  for the component  $i$ :

$$NLL = \sum_{i=1}^{n_s} \sum_{t=1}^{n_t} -\log L(\theta_i^t | RUL_i^{*(0:t)}). \quad (3)$$

### 3. Investigation methodology

This section aims to present the methodology to investigate the capacity of PDL for handling uncertainties in RUL predictions. Subsection 3.1 describes the design of numerical experiments while subsection 3.2 presents the metrics used to evaluate the point-wise accuracy and the uncertainty management capacity of the investigated models.

#### 3.1. Description of numerical experiments

Without loss of generality, let's assume that there exist components whose degradation process follows stochastic processes. The component is failed when its degradation level exceeds  $L = 80$ . The experimental setup is illustrated in Figure 2. To simulate the run-to-failure processes, 200 degradation trajectories are generated using the homogeneous gamma (HGP) and non-homogeneous gamma process (NHGP), with a time step of 0.2-time units (t.u). The parameters

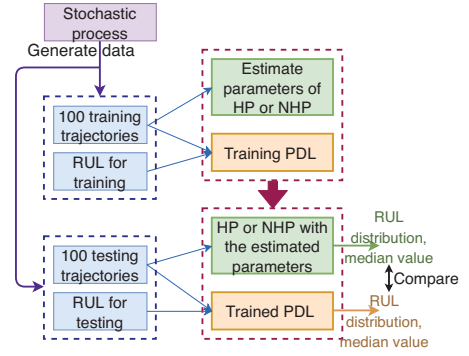


Fig. 2.: Design of numerical experiments.

HG, NHG, and PDL refer to homogeneous gamma process, non-homogeneous gamma process, and probabilistic deep learning.

of HP and NHGP are selected in such a way that their mean value of the degradation level at  $t = 100$  is 100 with the coefficients of variation (CV) set to 10%, 30%, and 50% respectively. The corresponding parameters are listed in Table 1.

Table 1.: Parameters of stochastic processes.

	HGP	NHGP	NHWP
$CV = 10\%$	$a = 1, b = 1$	$b = 1, a = 0.01, c = 2$	$e = 0.01, f = 2$
$CV = 30\%$	$a = 0.11, b = 0.11$	$b = 0.11, a = 0.001, c = 2$	$e = 0.09, f = 0.22$
$CV = 50\%$	$a = 0.04, b = 0.04$	$b = 0.04, a = 0.0001, c = 2$	$e = 0.25, f = 0.08$

Among 200 components' degradation trajectories, 100 trajectories are employed to estimate the parameters of the corresponding HGP and NHGP process and also to train PDL models as presented in Section 2. The configuration parameters of the PDL models are presented in Table 2.

Table 2.: PDL models' configuration parameters.

1 <sup>st</sup> LSTM (or GRU) layer	2 <sup>nd</sup> LSTM (or GRU) layer	Dropout	Learning rate
100 units	50 units	0.2	0.001

For testing, the remaining 100 trajectories are used to evaluate the capacity of PDL in handling prognostic uncertainties. Specifically, we compare the RUL distribution and its median value

obtained by PDL with those of the HGP and NHGP processes corresponding to the stochastic data under consideration. Note that for the testing phase, the 100 run-to-failure trajectories are randomly truncated before reaching their failure time, as illustrated in Figures 3 and 4. In addition, to evaluate the adaptability of PDL in predicting RUL when degradation data is produced by non-Gamma processes, we keep the architecture and configuration parameters of the PDL models and train them with degradation data generated by the non-homogeneous Wiener process (NHWP). Its independent increments are given by  $dX_t = \mu(t)dt + \sigma(t)dB_t$ , where  $\mu(t) = fet$ ,  $\sigma(t) = \sqrt{2et}$ , and  $B_t$  denotes a standard Brownian motion. The process parameters (shown in Table 1) are selected such that their mean failure time is 100 t.u, with coefficients of variation (CV) set to 10%, 30%, and 50%, respectively. Note that the HGP and NHGP models cannot predict RUL in this case.

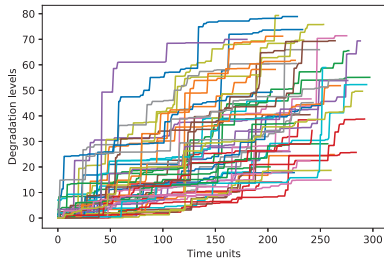


Fig. 3.: Testing data generated by HGP, CV=30%.

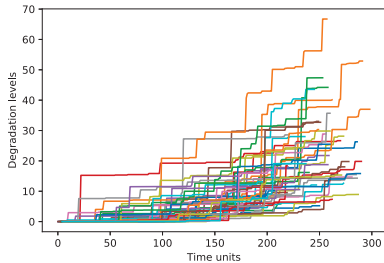


Fig. 4.: Testing data generated by NHGP, CV=30%.

### 3.2. Performance evaluation metrics

This section aims to present the metrics for performance evaluation of the investigated models on both aspects: point-wise prediction and uncertainty management.

#### 3.2.1. Point prediction accuracy metrics

Given  $M$  the total number of prediction points and  $d_k$  be the difference between the  $k$ -th actual ( $RUL_k^*$ ) and estimated ( $\hat{RUL}_k$ ) RUL values, the performance of prognostic models can be evaluated by the following point prediction accuracy metrics.

**Mean squared error (MSE):** MSE is a widely used metric to evaluate the point prediction accuracy Gugulothu et al. (2017) by the following formulation:

$$MSE = \frac{1}{M} \sum_{k=1}^M d_k^2 \tag{4}$$

where  $d_k = RUL_k^* - \hat{RUL}_k$ .

**Scoring function (SF):** SF, which is a popular metric used to evaluate the performance of prognostics algorithms Gugulothu et al. (2017), allows punishing late prediction more heavily than an early prediction, as defined below,

$$SF = \frac{1}{M} \sum_{k=1}^M s_k; s_k = \begin{cases} e^{-\frac{d_k}{13}} - 1, & \text{if } d_k < 0 \\ e^{\frac{d_k}{10}} - 1, & \text{if } d_k \geq 0 \end{cases} \tag{5}$$

#### 3.2.2. Uncertain prediction evaluation metrics

**PICP:** Prediction interval coverage percentage (PICP) is widely used in literature Gao et al. (2020). It represents the probability that the true targets ( $RUL_k^*$ ) fall within the lower and upper bounds ( $[L_\alpha(RUL_k), U_\alpha(RUL_k)]$ ) of predictions,  $RUL_k$ , with a prescribed confidence level  $(1 - \alpha)$ . It is given by:  $PICP = \frac{1}{M} \sum_{k=1}^M I(RUL_k^*)$  where

$$I(RUL_k^*) = \begin{cases} 1, & \text{if } RUL_k^* \in [L_\alpha(\hat{RUL}_k), U_\alpha(\hat{RUL}_k)] \\ 0, & \text{if } RUL_k^* \notin [L_\alpha(\hat{RUL}_k), U_\alpha(\hat{RUL}_k)] \end{cases}$$

Note that the performance of the prediction model is better when the values of SF and MSE are smaller while the accuracy PICP is greater.

## 4. Result analysis

The presented results in Table 3 compare the performance of different models in predicting RUL of the components whose degradation evolution follows the homogeneous gamma process (HGP). Three evaluation metrics have been used to assess the performance of the models, including RMSE,

Table 3.: Testing results for data generated by homogenous gamma process.

CV	Model	RMSE	SF	PICP
<b>10%</b>	HGP	5.53	0.53	0.85
	LSTM + WB	5.99	0.58	0.99
	GRU + WB	6	0.64	0.99
	LSTM + LN	6.29	0.72	0.86
	GRU + LN	6.53	0.78	0.88
<b>30%</b>	HGP	29.88	15.76	1
	LSTM + WB	20.18	6.72	0.97
	GRU + WB	19.87	7.14	0.98
	LSTM + LN	23.99	11.69	0.95
	GRU + LN	21.40	7.76	0.92
<b>50%</b>	HGP	42.7	710	1
	LSTM + WB	53.51	1636.79	0.89
	GRU + WB	54.55	1159.03	0.86
	LSTM + LN	54.95	931.908	0.87
	GRU + LN	54.11	919.773	0.86

Table 4.: Testing results for data generated by nonhomogenous gamma process.

CV	Model	RMSE	SF	PICP
<b>10%</b>	NHGP	4.26	0.37	0.93
	LSTM + WB	5.54	0.63	1
	GRU + WB	5.49	0.63	0.98
	LSTM + LN	4.75	0.50	0.91
	GRU + LN	5.37	0.60	0.81
<b>30%</b>	NHGP	13.66	1.99	0.93
	LSTM + WB	12.32	2.30	0.94
	GRU + WB	11.35	1.94	0.93
	LSTM + LN	11.78	1.92	0.93
	GRU + LN	11.79	1.91	0.93
<b>50%</b>	NHGP	23.03	7.79	0.91
	LSTM + WB	25.71	14.01	0.91
	GRU + WB	25.26	20.78	0.92
	LSTM + LN	28.25	28.52	0.89
	GRU + LN	29.01	27.59	0.97

SF, and PICP. The lower the value of RMSE and SF, the better the point-wise accuracy of the models. However, for PICP, the higher its value, the better the model’s uncertainty management ability.

The results show that HGP is the best suitable model for predicting RUL in the dataset generated by HGP. However, all PDL models (LSTM + WB, GRU + WB, LSTM + LN, and GRU + LN) demonstrate sufficiently good performance for all three levels of the coefficient of variation (10%, 30%, and 50%). Among the PDL models, LSTM + WB and GRU + WB perform better than LSTM + LN and GRU + LN for all three levels of the coefficient of variation. It is also noteworthy that as the coefficient of variation increases, the models’ performance decreases, which implies that predicting RUL becomes more challenging in more variable conditions.

The results presented in Table 4 show that the PDL models outperform the NHGP when the coefficient of variation is 30%. For the coefficient of variation of 50%, the NHGP model outperforms all the PDL models for the RMSE and SF metrics, indicating its better ability to provide accurate point predictions. However, all PDL models provide comparable results, especially for PICP met-

rics, indicating their ability to manage uncertainties. It is interesting to note that the PDL models based on LSTM and GRU perform similarly and that the choice of probability distribution (Weibull or Lognormal) does not significantly affect the performance of the models.

The results presented in Table 5 demonstrate the adaptability of PDL for predicting RUL in degradation data generated by the nonhomogenous Wiener process. It is important to note that the HGP and NHGP models are not suitable for predicting RUL in this case due to the possibility of negative increments in the degradation process. For the dataset with a coefficient of variation of 10%, all PDL models achieved good results. As the coefficient of variation increases to 30% and 50%, the performance of the PDL models decreases, with higher RMSE and SF values and lower PICP values. Among them, LSTM + WB shows the best performance for this dataset according to PICP metrics. However, none of the PDL models display superior point-wise accuracy compared to the others, in all scenarios.

In summary, the findings in this section show that the selection of DL architecture (LSTM or GRU) and the choice of probability distribution

Table 5.: Testing results for data generated by nonhomogenous Wiener process.

CV	Model	RMSE	SF	PICP
10%	LSTM + WB	4.57	0.4	0.98
	GRU + WB	4.41	0.43	0.96
	LSTM + LN	4.61	0.43	0.93
	GRU + LN	4.41	0.44	0.96
30%	LSTM + WB	14.56	3.29	0.95
	GRU + WB	13.34	2.43	0.92
	LSTM + LN	13.98	2.72	0.84
	GRU + LN	13.33	2.37	0.91
50%	LSTM + WB	20.14	9.94	0.93
	GRU + WB	21.55	14.16	0.88
	LSTM + LN	22.62	14.3	0.84
	GRU + LN	21.31	17.54	0.85

(Weibull or Lognormal) do not significantly influence the performance of PDL models. This emphasizes the potential of PDL models in effectively managing uncertainties associated with RUL predictions. In fact, in cases where the degradation process is not well understood, a PDL model can be applied without a strict requirement to select a specific DL architecture or probability distribution, while still achieving sufficiently accurate results.

## 5. Discussion and conclusion

This study has investigated the capacity of PDL models to manage uncertainty in predicting RUL relative to several stochastic processes by assuming a sufficient set of trajectories to train the models. The performance of each model was assessed using specific criteria. The results indicate that PDL models are capable of handling temporal uncertainty when data are generated from Gamma and Wiener processes. Furthermore, the selection of DL architecture (LSTM or GRU) and probability distribution (Weibull or Lognormal) did not significantly affect the performance of PDL models. This highlights the potential of PDL models to effectively manage uncertainties associated with RUL predictions, especially in cases where the degradation process is not well understood. The ability to apply a PDL model without

the need for a specific DL architecture or probability distribution can reduce the risk of making incorrect decisions, such as safety problems or high maintenance costs Al Masry et al. (2017b). The advantages and disadvantages of PDL models and stochastic processes for handling RUL uncertainty are summarized in Table 6. Additionally, some stochastic processes, such as extended gamma processes Al Masry et al. (2017a) and transformed gamma process Giorgio et al. (2018), may be challenging to implement in practice. Future research may focus on applying PDL models to extended and transformed gamma processes and extending the methodology to account for statistical dependencies between components.

## References

- Al Masry, Z., S. Mercier, and G. Verdier (2017a). Approximate simulation techniques and distribution of an extended gamma process. *Methodology and Computing in Applied Probability* 19, 213–235.
- Al Masry, Z., S. Mercier, and G. Verdier (2017b). A condition-based dynamic maintenance policy for an extended gamma process. In *MMR 2017 (International Conference on Mathematical Methods on Reliability)*.
- Cho, K., B. van Merriënboer, C. Gulcehre, F. Bougares, H. Schwenk, and Y. Bengio (2014). Learning phrase representations using rnn encoder-decoder for statistical machine translation. In *Conference on Empirical Methods in Natural Language Processing (EMNLP 2014)*.
- Dhada, M., A. K. Parlikad, O. Steinert, and T. Lindgren (2023, February). Weibull recurrent neural networks for failure prognosis using histogram data. *Neural Computing and Applications* 35(4), 3011–3024.
- Gao, G., Z. Que, and Z. Xu (2020). Predicting remaining useful life with uncertainty using recurrent neural process. In *2020 IEEE 20th International Conference on Software Quality, Reliability and Security Companion (QRS-C)*, pp. 291–296. IEEE.
- Giorgio, M., M. Guida, and G. Pulcini (2018). The transformed gamma process for degradation phenomena in presence of unexplained

Table 6.: Stochastic process vs probabilistic deep learning for RUL prediction.

Model	Stochastic process	Probabilistic deep learning
Requirements	Strict assumptions on increments Parameter estimation Goodness-of-fit test	No strict requirement to select a specific deep learning architecture Hyper-parameters selection
Advantages	Distributional RUL Handle uncertainty Capture degradation mechanism Predict the future degradation Few observations	Distributional RUL Handle Uncertainty No need for model selection Adaptability to numerous stochastic process like HGP, NHGP and Wiener
Disadvantages	Specific degradation behavior Difficulty of parameter estimation Wrong model assumption Explicit formula for RUL distribution	Time consuming for training phase Difficulty of hyper-parameters optimization Large set of observations

forms of unit-to-unit variability. Quality and Reliability Engineering International **34**(4), 543–562.

Gugulothu, N., V. TV, P. Malhotra, L. Vig, P. Agarwal, and G. Shroff (2017, September). Predicting Remaining Useful Life using Time Series Embeddings based on Recurrent Neural Networks. [arXiv:1709.01073 \[cs\]](https://arxiv.org/abs/1709.01073).

Hinton, G. E., N. Srivastava, A. Krizhevsky, I. Sutskever, and R. R. Salakhutdinov (2012). Improving neural networks by preventing co-adaptation of feature detectors. [arXiv preprint arXiv:1207.0580](https://arxiv.org/abs/1207.0580), 1–18.

Hochreiter, S. and J. Schmidhuber (1997). Long short-term memory. Neural computation **9**(8), 1735–1780.

Kahle, W., S. Mercier, and C. Paroissin (2016). Degradation processes in reliability. John Wiley & Sons.

Liu, C., L. Zhang, Y. Liao, C. Wu, and G. Peng (2019). Multiple sensors based prognostics with prediction interval optimization via echo state gaussian process. IEEE Access **7**, 112397–112409.

Nguyen, K. T., M. Fouladirad, and A. Grall (2018). Model selection for degradation modeling and prognosis with health monitoring data. Reliability Engineering & System Safety **169**, 105–116.

Nguyen, K. T. and K. Medjaher (2019). A new

dynamic predictive maintenance framework using deep learning for failure prognostics. Reliability Engineering & System Safety **188**, 251–262.

Nguyen, K. T., K. Medjaher, and C. Gogu (2022). Probabilistic deep learning methodology for uncertainty quantification of remaining useful lifetime of multi-component systems. Reliability Engineering System Safety **222**, 108383.

Nguyen, K. T. P., K. Medjaher, and D. T. Tran (2022, September). A review of artificial intelligence methods for engineering prognostics and health management with implementation guidelines. Artificial Intelligence Review.

Paroissin, C. and A. Salami (2014). Failure time of non homogeneous gamma process. Communications in Statistics-Theory and Methods **43**(15), 3148–3161.

van Noortwijk, J. M. (2009). A survey of the application of gamma processes in maintenance. Reliability Engineering & System Safety **94**(1), 2–21.

Zhang, S.-J., R. Kang, and Y.-H. Lin (2021, April). Remaining useful life prediction for degradation with recovery phenomenon based on uncertain process. Reliability Engineering & System Safety **208**, 107440.